ELSEVIER

Contents lists available at ScienceDirect

### Ceramics International

journal homepage: www.elsevier.com/locate/ceramint



## Insight into the evolution mechanism of carbon film and Eu valence in carbon coated BaMgAl<sub>10</sub>O<sub>17</sub>: Eu<sup>2+</sup> phosphor annealed in air



Liang-Jun Yin<sup>a,1</sup>, Wen-Jie Xie<sup>b,1</sup>, Meng Wang<sup>a,1</sup>, Wei Tian<sup>a,1</sup>, Sheng-Hui Zhang<sup>a</sup>, Ying-Lin Liang<sup>c</sup>, Ming-Hsien Lee<sup>d</sup>, Ming-zhen Liu<sup>e</sup>, Xian Jian<sup>a,\*</sup>, Long-Jiang Deng<sup>f,\*</sup>

- a School of Materials and Energy, University of Electronic Science and Technology of China, 2006 Xiyuan Road, Chengdu 611731, PR China
- <sup>b</sup> School of Materials and Chemical Engineering, Anhui Jianzhu University, Hefei, PR China
- <sup>c</sup> School of Mechatronics Engineering, University of Electronic Science and Technology of China, 2006 Xiyuan Road, Chengdu 611731, PR China
- <sup>d</sup> Department of Physics, Tamkang University, Tamsui, New Taipei 25137, Taiwan
- <sup>e</sup> Center for Applied Chemistry, University of Electronic Science and Technology of China, Chengdu 611731, PR China
- f National Engineering Research Center of Electromagnetic Radiation Control Materials, University of Electronic Science and Technology of China, 2006 Xiyuan Road, Chengdu, PR China

#### ARTICLE INFO

# Keywords: Coating Oxidation resistance BAM phosphor Reduction Luminescence

#### ABSTRACT

Performing carbon coating on the surface of phosphors has been proven to be an effective strategy to enhance the oxidation resistance, which is an important factor to achieve stable luminescent devices. Therefore, a good understanding of the protection mechanism favors a continuous improvement of oxidation resistance of phosphors. In present paper, the evolution of the carbon layer, Eu valence (Eu<sup>2+</sup>/Eu<sup>3+</sup>), and luminescent properties for the C coated BaMgAl<sub>10</sub>O<sub>17</sub>: Eu<sup>2+</sup> phosphor when annealed at high temperature is investigated carefully. Decrease of carbon layer promotes the appearance color transition from black to white as the annealing temperature rises to 1000 °C in air. As expected, the decrease of carbon layer will enhance the luminescence intensity, but risk the possible oxidation of Eu<sup>2+</sup> to Eu<sup>3+</sup>, which inhibits the blue emission ascribed to Eu<sup>2+</sup>. The results indicate that luminescence intensity of phosphor is dependent on the synergistic effect of carbon thickness and Eu<sup>2+</sup>/Eu<sup>3+</sup> ratio. Additionally, a reduction reaction of Eu<sup>3+</sup> to Eu<sup>2+</sup> is observed in C coated BaMgAl<sub>10</sub>O<sub>17</sub>: Eu<sup>2+</sup> phosphor when annealed at high temperature, which also contributes to the higher luminescence intensity.

#### 1. Introduction

As a commercial blue phosphor,  ${\rm Eu}^{2+}$  doped  ${\rm BaMgAl_{10}O_{17}}$ :  ${\rm Eu}^{2+}$  (BAM) owns high quantum efficiency (external quantum efficiency up to 65%), good chromaticity and strong absorption capacity in the (vacuum) ultraviolet excitation band, making it widely used in three-band fluorescence lamps and white light-emitting diode (LED) [1–4].

In the practical application of luminescent devices, much heat will be generated. It is a challenging task for phosphors to remain the same luminescent efficiency after long-term working because  $Eu^{2+}$  luminescent ions are easily oxidized to  $Eu^{3+}$  at high temperature in the air, which will reduce the luminescent efficiency irreversibly. As for BAM, it exhibits a layered structure in which  $Eu^{2+}$  ions are sandwiched between the spinel blocks. As a result,  $Eu^{2+}$  ions are thus easily oxidized. The oxidation takes place in the following steps: the adsorption of  $O_2$  at the phosphor surface followed by incorporation of an oxygen atom into

an oxygen vacancy; diffusion of  $\mathrm{Eu}^{2+}$  ions along the conduction layer; the electron transfer from a  $\mathrm{Eu}^{2+}$  ion to the incorporated oxygen atom, resulting the transformation of  $\mathrm{Eu}^{2+}$  to  $\mathrm{Eu}^{3+}$ . Plenty of previous research indicates that the BAM phosphor undergoes a decrease of luminescence intensity when baked in air or irradiated by ultraviolet photons/ion sputtering. Notably, BAM phosphor will suffer from serious luminescence degradation due to the oxidation of luminescent  $\mathrm{Eu}^{2+}$  centers when the heating temperature rises to 500 °C [4–7]. This kind of degradation is general for other phosphors. Similar cases are also addressed in  $\mathrm{Sr}_2\mathrm{Si}_5\mathrm{N}_8$ :  $\mathrm{Eu}^{2+}$  and  $\mathrm{Sr}_{\mathrm{Si}_2\mathrm{O}_2\mathrm{N}_2}$ :  $\mathrm{Eu}^{2+}$  phosphors [8,9].

In order to solve this issue, many methods like surface coating, doping other ions and heat-treatment in inert atmosphere have been proposed so far to enhance the oxidation resistance of BAM phosphor. [5,10–16] Among them, depositing a thin layer on the surface of phosphor particle is an easily operational and effective methodology to improve the chemical stability of BAM phosphor [16–19]. At high

Corresponding authors.

E-mail addresses: jianxian@uestc.edu.cn (X. Jian), denglj@uestc.edu.cn (L.-J. Deng).

<sup>1</sup> co-first authors

temperature in air, the thin layer can prevent  $O_2$  penetration and oxidation attack to the phosphor, which favors the better thermal stability of BAM. Interestingly, our previous research achieved a thin C coating on the surface by CVD method. It was found that the luminescent efficiency was not affected when the coating layer is limited to 1–5 layers due to high light transmittance up to 97.7% for single graphene layer in the ultraviolet-visible spectrum [20,21]. Unfortunately, the specific change of the structure, composition and protection mechanism for the C@BAM phosphor at high temperature is still unknown. This work focuses on the evolution of carbon film, Eu valence and luminescent properties in the thermal treatment of the C@BAM phosphor in the air. Some intriguing results from XANES, TGA, HRTEM and PL motivate us to further understand the thermal-resistance mechanism of other C coated phosphors.

#### 2. Experimental section

BAM powders were prepared by solid-state reaction from starting mixtures of BaCO<sub>3</sub>, MgO, Al<sub>2</sub>O<sub>3</sub> and Eu<sub>2</sub>O<sub>3</sub> (99.99 wt%, Sinopharm Chemical Reagent Co. Ltd) in N<sub>2</sub> atmosphere at 1500 °C for 3 h. Carbon coated BAM was prepared at 700 °C under gas mixtures of N<sub>2</sub> (gas flow rate: 100 ml/min) and C<sub>2</sub>H<sub>2</sub> (gas flow rate: 30 ml/min). The details are: (i) BAM powders were put in the quartz boat; (ii) The temperature of the furnace was raised to 700 °C and hold stable for 30 mins under N<sub>2</sub> atmosphere (gas flow rate: 100 ml/min); (iii) C<sub>2</sub>H<sub>2</sub> gas (gas flow rate: 30 ml/min) was introduced into the tube for 5 mins; (iv) C@BAM was obtained after natural cooling of the sample in the furnace under N<sub>2</sub> atmosphere. To investigate the effect of thermal treatment on carbon film, Eu valence and luminescent properties, obtained C@BAM powders were further annealed in the air.

The phase formation was analyzed by an X-ray diffractometer (Model PW 1700, Philips, Eindhoven, The Netherlands) using Cu Ka radiation at a scanning rate of 2°/min. The inner structure was observed by Transmission Electron Microscopy (TEM) equipped with Energy Dispersion X-ray (EDX) spectrometer (Model 2100 F, JEOL, Tokyo, Japan). A Mettler Toledo Thermo-Gravimetric Analyzer (TGA 851e) was used to study the thermal stability behavior of the synthesized powders. The TGA-DTA curves were recorded while ramping up the powders from 25 °C to 1000 °C with a ramping rate of 5 °C min<sup>-1</sup> in a air flow of 100 ml/min. The photoluminescence spectra were measured by a fluorescence spectrophotometer (Model F-4600, Hitachi, Tokyo, Japan) with a 200 W Xe lamp as an excitation source. The emission spectrum was corrected for the spectral response of the monochromator and Hamamatsu R928P photomultiplier tube (Hamamatsu Photonics K.K., Hamamatsu, Japan) by a light diffuser and tungsten lamp (Noma Electric Corp., NY; 10 V, 4A). The excitation spectrum was also corrected for the spectral distribution of the Xe lamp intensity by measuring Rhodamine-B as a reference. The diffuse-reflectance spectra were measured at room temperature by a UV-Vis-NIR spectrophotometer (Model CARY 5000, Agilent Technologies, USA) equipped with an integrating sphere (Model Internal DRA-2500, Agilent Technologies, USA).

#### 3. Results and discussions

As for the prepared carbon-coated BAM phosphor (C@BAM), it shows black appearance, as shown in Fig. 1-a, indicating that the thick carbon layer almost absorbs the whole visible light in the natural environment. Considering the thermodynamic property, carbon is prone to react with  $O_2$  and forms  $CO_2$  gas under high temperature conditions, followed by releasing into air. Therefore, performing annealing in air will exhaust carbon, which promotes the appearance transition of C@BAM. Especially, annealing at higher temperature accelerates the oxidation reaction and removes more carbon from C@BAM, resulting in the color change of the powders from black to white as the temperature rises. With respect to the annealing effect on the carbon coated

phosphor as seen in Fig. 1-a, the black phosphor gradually becomes grey and then white as increasing the annealing temperature from room temperature to 1000 °C for 2 h in air atmosphere. Notably, samples annealed at temperature higher than 600 °C exhibit almost equally white powders, suggesting that the remained carbon layer is quite thin or even completely disappeared due to the oxidation of carbon in the air. For simplicity, we will name the annealed samples as C@BAM-400 °C, C@BAM-600 °C, C@BAM-700 °C, C@BAM-800 °C and C@BAM-1000 °C in the remainder of this paper. Uncoated white BAM doesn't show appearance transition when annealed at the temperature of 25–1000 °C, whose images are not exhibited in present research.

Under 365 nm light irradiation, a weak blue emission is still present in the prepared black C@BAM, which is definitely ascribed to  $Eu^{2+}$  luminescence in BAM. As increasing the annealing temperature, more carbon is removed from C@BAM. As a result, a stronger luminescence intensity is emitted and reaches its peak in C@BAM-700 °C sample. However, the intensity gradually starts to decrease in C@BAM-800 °C and C@BAM-1000 °C samples. The PL results can be found in Fig. 1-b, c, which matches well with visual observation under 365 nm excitation. For uncoated BAM, the emission intensity gradually decreases as the increase of the heat-treatment temperature (Fig. 1-c), which is linked to the decrease of the  $Eu^{2+}$  ion concentration in BAM caused by the oxidation of  $Eu^{2+}$  to  $Eu^{3+}$ .

The shape of excitation and emission spectra seems similar between BAM and C@BAM samples with the increase of annealing temperature. These detailed PL results can be found in Fig. SI-1 in the Supporting information. The XRD patterns of all the annealed BAM and C@BAM samples don't show any discrepancy, as seen in Fig. SI-2 in the Supporting information. The above conclusions indicate the unchanged crystal structure of BAM even if carbon-coating or heat-treatment is introduced.

Actually, the emission intensity of annealed C@BAM is controlled by the carbon thickness and oxidation degree of  $Eu^{2+}$  to  $Eu^{3+}$ . Thick carbon layer will absorb the incident and emitted light. Oxidation of  $Eu^{2+}$  to  $Eu^{3+}$  will reduce the luminescent centers. Both factors lead to the degradation of final emission intensity. As increasing the heattreatment temperature, carbon layer becomes thin, which helps to release photons and enhance the emission intensity. However, in this situation, it is expected that the oxidation of  $Eu^{2+}$  to  $Eu^{3+}$  will be strengthened, which inhibits the emission intensity. So the carbon thickness and Eu valence determine the final luminescence intensity. In following part, we will talk about the individual factor, respectively.

Energy-dispersive X-ray spectrometry (EDS) mapping analysis performed on C@BAM sample is shown in Fig. 2-a. The Ba, Mg, Al, O, Eu atom signals observed in the same concentrated area represent the prepared BAM crystal. The distribution of carbon shapes a thin layer around the BAM particle indicating the carbon coating on the surface of phosphor particles. HRTEM image of C@BAM as seen in Fig. 2-b suggests that the coating is nearly composed of 16 carbon layers. FFT pattern in Fig. 2-c reveals that the deposited carbon layers show the nature of partial graphitization. As seen in the HRTEM images of Fig. 2, it can be visualized that the heat-treatment does cause significant changes in the carbon layers, including the layer thickness and morphology. The carbon layer of C@BAM becomes thinner as a result of the oxidation in the air. Specifically, carbon layer decreases from 16 layers in the starting C@BAM to 3-4 layers in the C@BAM-600 °C (Fig. 2-e), then to 1-2 layers in the C@BAM-700 °C (Fig. 2-f). It should be noted that carbon is absent in some part of C@BAM-700 °C, as seen in the amplified fine structure (indicated by dotted rectangles). After thermal treatment, the remained carbon is clearly non-uniform, where some voids and pores are formed by the escaping gases as observed in the amplified fine structure, which indicates the oxidation of carbon according to the reaction:  $2C(s) + O_2(g) \rightarrow 2CO_2(g)$ . No trace of carbon is observed in C@BAM-800°C (Fig. 2-g) and C@BAM-1000°C (not shown), indicating the complete disappearance of carbon under this annealing temperature.

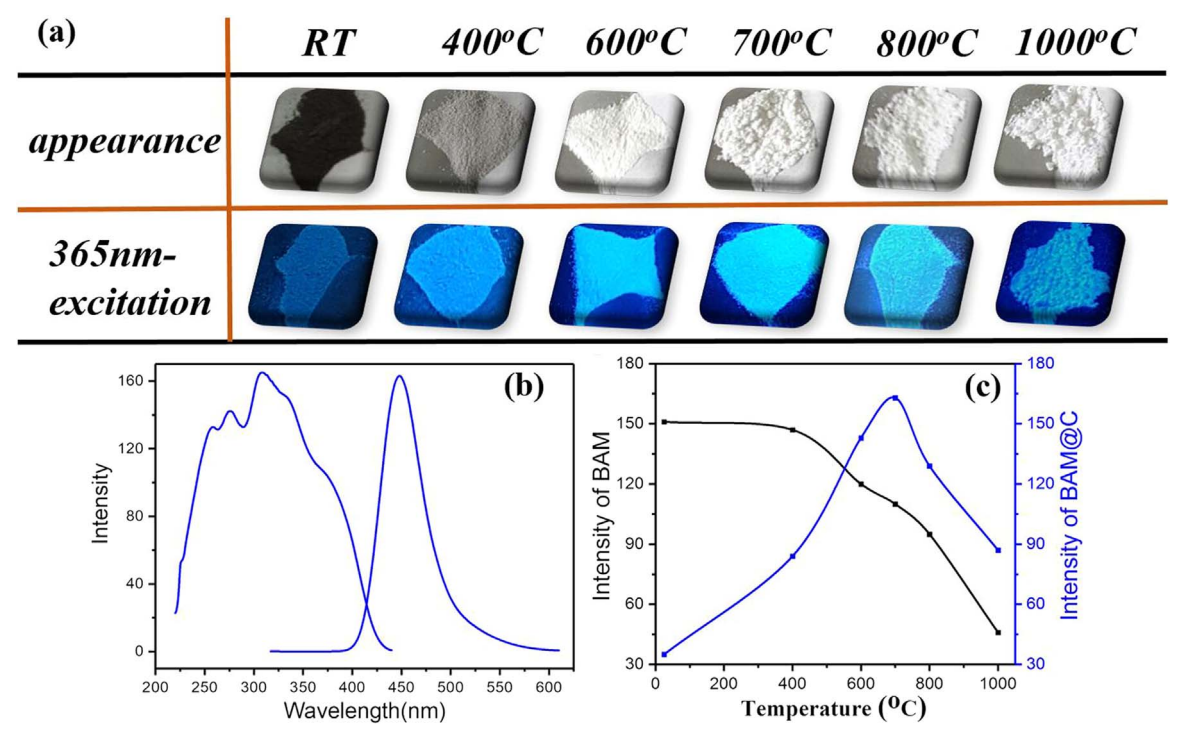


Fig. 1. (a) Images of C@BAM samples after annealed at 25–1000 °C for 2 h in air with and without UV-365 nm irradiation; (b) PL spectra for C@BAM-700 °C as an example; (c) Maximal Emission intensity under 310 nm excitation for BAM and C@BAM as a function of annealing temperature.

As mentioned in the HRTEM images, the carbon layers are made up of multi-layer graphene. It has been widely reported that single layer graphene can reach ultraviolet-visible light transmittance up to 97.7% theoretically [20,21]. In other words, light transmittance will decrease by 2.3% per layer with increase of carbon layers. Considering the C@ BAM, the final light transmittance of samples depends on the carbon layer number. The prepared C@BAM is black, which is caused by the extensive absorption of the thick carbon layer (16 layers) deposited on the surface of BAM powders. Light transmittance is enhanced with the decrease of carbon layers when C@BAM is annealed in the air. It explains the color transition of the powders from black to white as the annealing temperature increases. However, it will not have much impact on the absorption of the phosphor if carbon layer is limited to low thickness, i.e. 1-5 layers. Consequently, the appearance of C@BAM-600 °C and C@BAM-700 °C with 1-4 remained carbon layers is white, similar to carbon-free C@BAM-800 °C and C@BAM-1000 °C samples. According to previous reports, it suggests that 3-5 carbon layers result in the best luminescence intensity of C@BAM due to the surface modification [22]. Moreover, high temperature annealing risks the higher oxidation of Eu<sup>2+</sup> to Eu<sup>3+</sup>. It is expected that C@BAM-600 °C should exhibit higher luminescence intensity than C@BAM-700 °C. However, a slight increase of luminescence intensity is observed in @BAM-700 °C compared with that in C@BAM-600 °C. There should be some other points to favor the enhanced luminescence intensity in C@BAM-700 °C sample.

In the annealing process,  $Eu^{2+}$  is easily attacked by  $O_2$  in the air and oxidized to  $Eu^{3+}$ , which can be reflected by XANES spectra. Fig. 3 shows the evolution of Eu valence in BAM and C@BAM samples with the increase of annealing temperature in the air. As shown in the Eu L<sub>3</sub>-edge XANES spectra, two peaks are present at about 6977 and 6984 eV, which correspond to the divalent and trivalent oxidation states of Eu, respectively. Both of non-heat-treated samples basically show the same characteristic that  $Eu^{2+}$  dominates, as seen in Fig. 3-(a) and (b). To be clearer, the relative ratios of the peak intensity at 6984 and 6977 eV ascribed to  $Eu^{3+}$  and  $Eu^{2+}$  in BAM and C@BAM are drawn in Fig. 3-(c) and (d). For the BAM,  $Eu^{2+}$  is gradually oxidized to  $Eu^{3+}$  when the annealing temperature increases, as seen in Fig. 3-(c). However, the

oxidation degree differs from each other in the C@BAM, as seen in Fig. 3-(d). Owing to the presence of carbon protection, there is no oxidation of  $\mathrm{Eu^{2}}^+$  happening at 400 °C. With the increase of the annealing temperature, slight oxidation is observed in C@BAM-600 °C. Although carbon still remains in the C@BAM-600 °C, which can theoretically support oxidation resistance, formed pores and defects in the carbon layer can expose the BAM to air and lead to oxidation of  $\mathrm{Eu^{2}}^+$ . Interestingly, an obvious anti-oxidation effect is observed in C@BAM-700 °C. It can be explained by the reduction effect of carbon, which can reduce the  $\mathrm{Eu^{3+}}$  to  $\mathrm{Eu^{2+}}$  according to the following formula.

$$C(s) + BAM:Eu^{3+}(s) \rightarrow CO(g) + BAM:Eu^{2+}(s)$$

That's why a reduction effect for the transformation of Eu<sup>3+</sup> to Eu<sup>2+</sup> is observed in the synthesis of other phosphors when raw materials mixed with carbon are heated in air [23]. It is suggested that this reduction reaction can happen at higher temperature, i.e. 700 °C instead of 600 °C. The XANES results mean that the reduction effect (Eu<sup>3+</sup> to Eu2+) dominates the oxidation effect (Eu2+ to Eu3+) for C@BAM-700 °C, finally resulting in the decrease of  $I_{Eu}^{3+}/I_{Eu}^{2+}$  value. The above HRTEM images for C@BAM-700 °C indicate that phosphor is not fully surrounded by carbon film. As a result, expanding annealing time will introduce more oxidation. In contrast to the PL intensity of C@BAM-700 °C, it decreases by 18% when as-prepared C@BAM sample is annealed for 3 h. It can be expected that reduction reaction dominates when the holding time is below 2 h, and oxidation reaction dominates when the holding time reaches 3 h. As for C@BAM-800 °C and C@BAM-1000 °C samples, carbon is completely fired and the oxidation becomes more serious. Therefore, higher amount of Eu3+ appears in C@BAM-800 °C and C@BAM-1000 °C samples.

Fig. 4 shows TGA-DTA curves of the BAM and C@BAM phosphors. Both of BAM and C@BAM undergo a weight loss when heated up to 400 °C. The weight loss can be ascribed to the release of absorbed water molecules [24]. Exceptionally, a slight weight gain in the BAM and C@BAM occurs at 240 °C probably due to the oxidation between phosphor and the absorbed oxygen molecules, which is consistent with the exothermic peak of DTA curves for both samples. Note that the weight growth is relatively small for the C@BAM, which can be ascribed to the

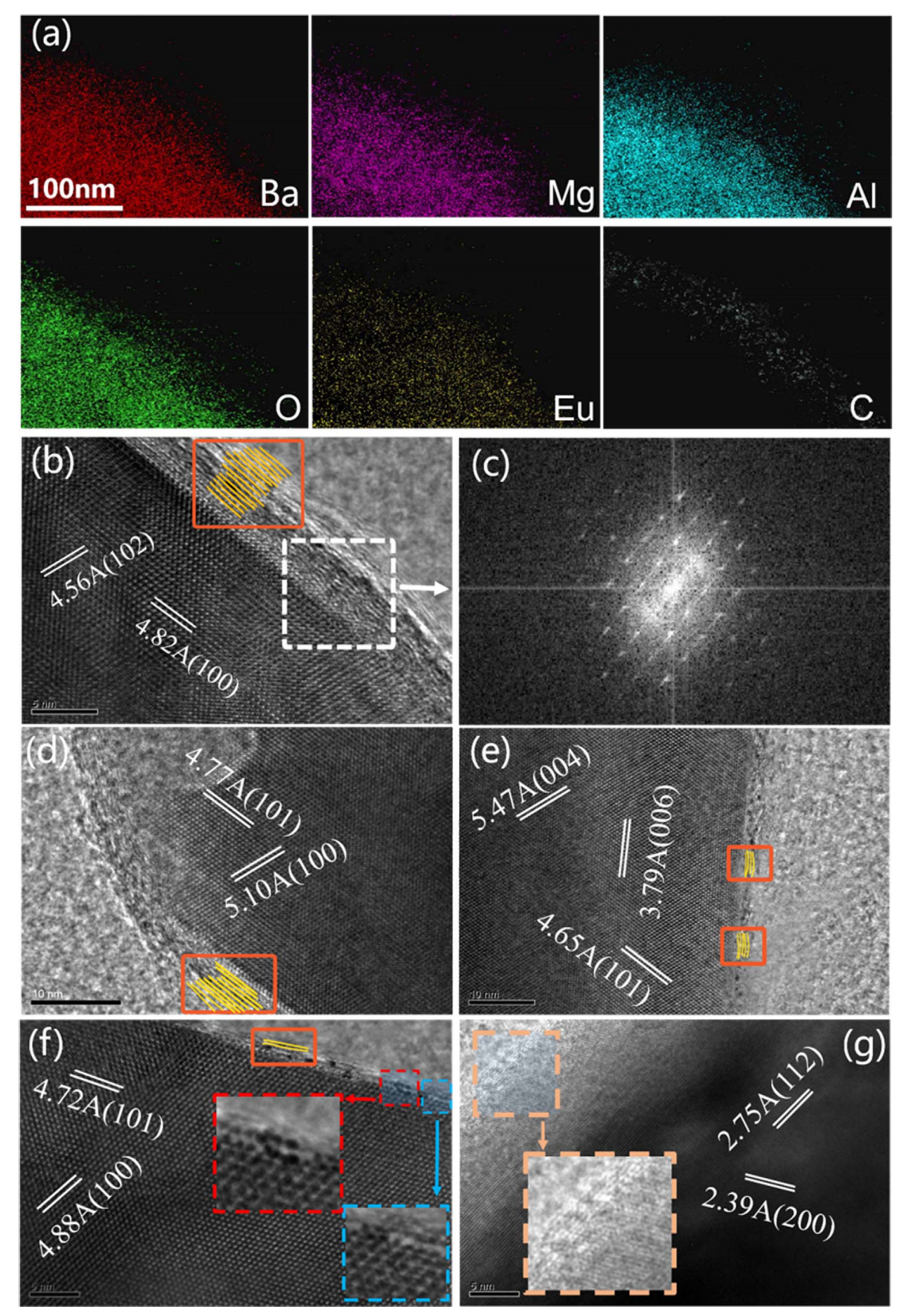


Fig. 2. (a) EDS mappings in C@BAM sample showing the distribution of Ba, Mg, Al, O, Eu and C elements, respectively. HRTEM images of annealed C@BAM samples under different temperature are shown, where (b), (d), (e), (f) and (g) represents TEM images of C@BAM, C@BAM-400 °C, C@BAM-600 °C, C@BAM-700 °C, C@BAM-800 °C, and FFT (c) corresponds to the area indicated by the square in (b).

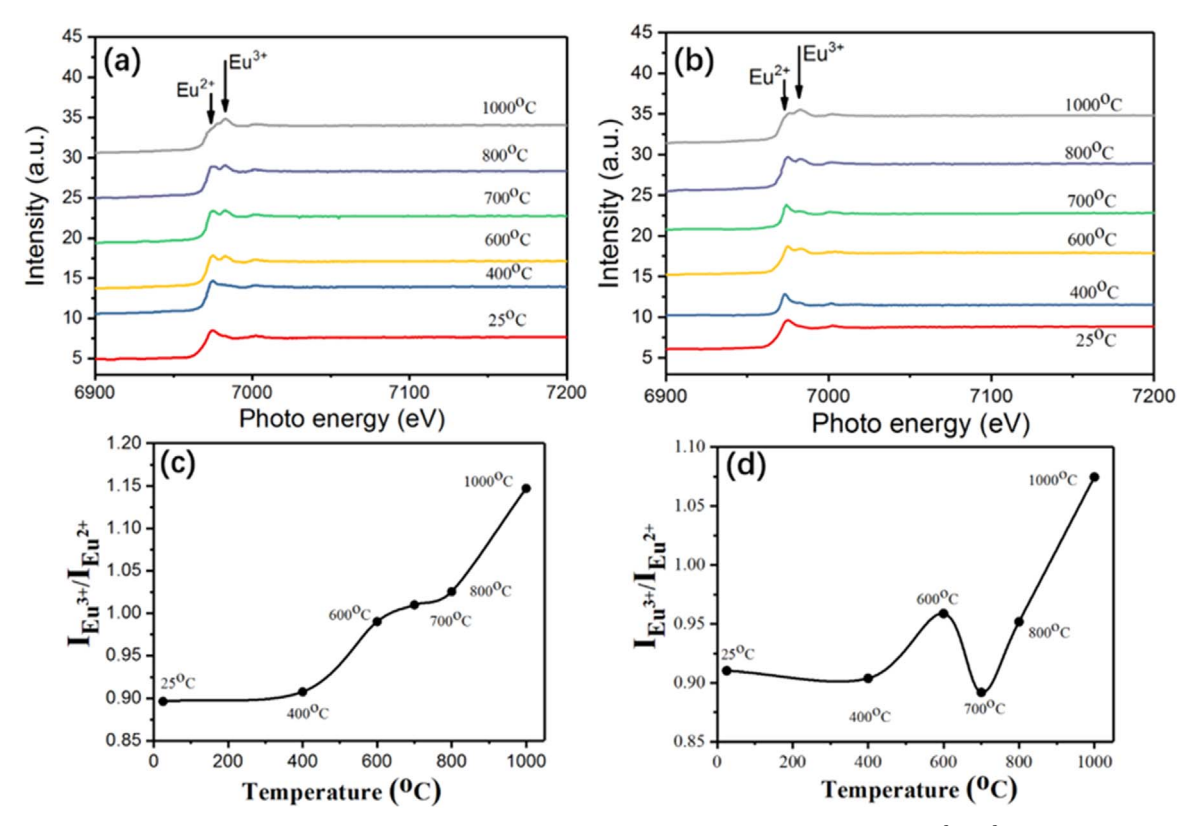


Fig. 3. Eu  $L_3$ -edge XANES spectra of BAM (a) and C@BAM (b) when annealed at different temperature in air. Figure (c) and (d) are the  $I_{Eu}^{3+}/I_{Eu}^{2+}$  ratios calculated from the peak value corresponding to  $Eu^{3+}$  and  $Eu^{2+}$  in Figure (a) and (b).

reduction of the absorbed oxygen molecules after carbon coating. Since temperature reaches to 600 °C, a weight gain of BAM is observed, which is attributed to the oxidation of the BAM phosphor when it is exposed to the air at high temperature. However, owing to the burning of deposited carbon on the surface of phosphor powders for C@BAM, a significant weight loss and an exothermic peak appears at 592 °C. The carbon burning lasts to 806 °C. It indicates that there is still some carbon remaining in the C@BAM - 800 °C, disagreed with the analyses of HRTEM results that carbon is absent in C@BAM - 800 °C. This inconsistency is caused by the different heating procedures between TGA measurement and long-time thermal treatment. As the temperature rises from 806 °C to 1000 °C, there is very minor weight increase due to its weakened oxidation. Compared with BAM, the C@BAM gains less weight, indicating that the C@BAM is more anti-oxidized. Therefore, we can come to a conclusion that the thermal stability of the C@BAM is

superior to that of BAM.

As known, thermal degradation shows a neglect effect in the practical use of luminescent devices. In order to minimize the thermal degradation, it is of great importance to protect phosphors from oxidation, which can be realized by carbon coating. Here, it has been proven that carbon coating can improve the stability of BAM phosphor and trigger the reduction reaction of  $\mathrm{Eu}^{3+}$  to  $\mathrm{Eu}^{2+}$  at high temperature. The evolution mechanism is schematically illustrated in detail, as seen in Fig. 5. Thus, the better performance of C@BAM may be attributed to the following reason: (1) compared with BAM, the oxygen molecule (O2) is not able to get adsorbed on the phosphor surface and subsequently be incorporated in the oxygen vacancy in C@BAM. Consequently, oxygen from the air will have few opportunities to oxidize  $\mathrm{Eu}^{2+}$  to  $\mathrm{Eu}^{3+}$ . This explains the higher thermal oxidation stability of C@BAM than that of BAM. (2) As increasing the annealing temperature, both BAM and C@

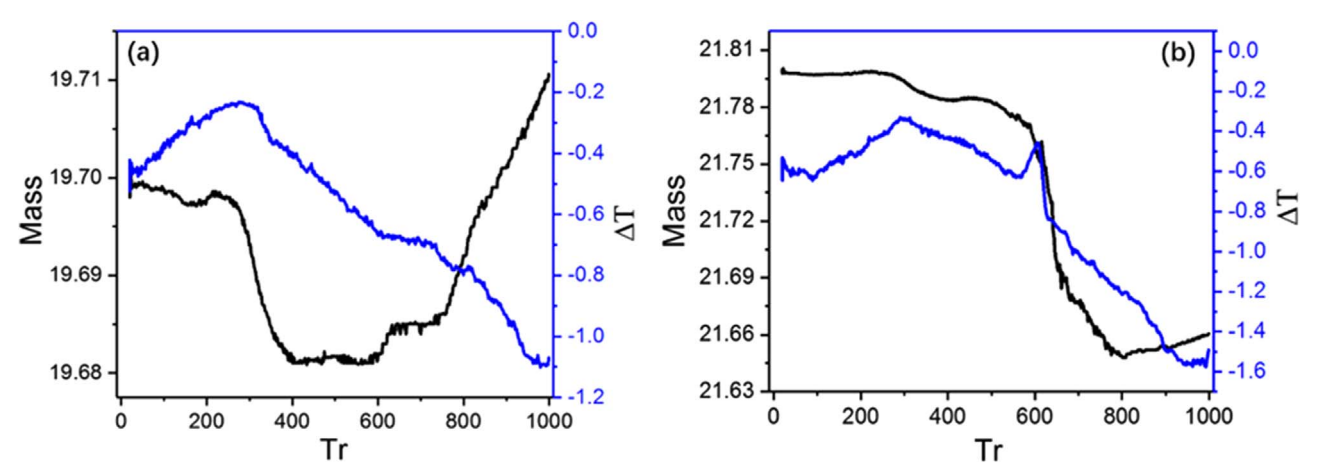


Fig. 4. TGA and DTA curves of the BAM (a) and C@BAM (b) heated in air.

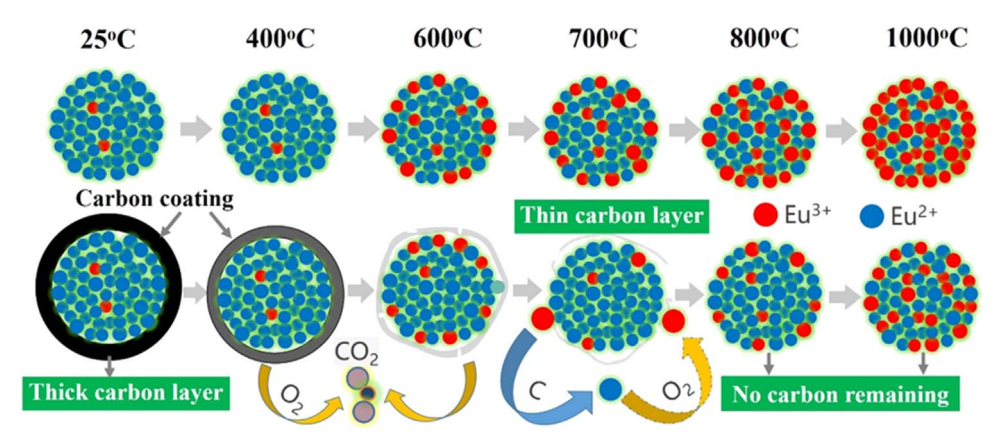


Fig. 5. A schematic picture showing evolution of carbon layer and oxidation degree in BAM and C@BAM annealed in air.

BAM expectedly suffer from higher oxidation of  $Eu^{2+}$  to  $Eu^{3+}$ . However, in C@BAM-700 °C, a reduction effect caused by carbon, reducing  $Eu^{3+}$  to  $Eu^{2+}$ , is observed. As a result, the luminescence intensity of C@BAM-700 °C is even superior to the starting BAM. Present conclusions provide us with a potential strategy to improve the luminescent performance of other carbon coated phosphors.

#### 4. Conclusion

In the process of thermal treatment in air, the structure and luminescent properties for the C coated BaMgAl<sub>10</sub>O<sub>17</sub>: Eu<sup>2+</sup> phosphor are researched systematically. Performing annealing on the black C@BAM phosphor with 16 carbon layers exhausts carbon and decreases the carbon layer, which results in appearance transition from black to white due to weakened light absorption of carbon. HRTEM and TGA-DTA results indicate that carbon burning starts at ~592 °C and lasts up to ~806 °C. Considering the negative light absorption of black carbon, the decrease of carbon layer to a certain number favors the enhanced luminescence intensity, but risks the possible oxidation of Eu<sup>2+</sup> to Eu<sup>3+</sup> inhibiting the blue emission of Eu<sup>2+</sup> when annealing temperature increases. Therefore, the total luminescence intensity of phosphors depends on the synergistic effect of carbon thickness and Eu<sup>2+</sup> oxidation degree. Compared to the continuous oxidation of  $\mathrm{Eu}^{2+}$  to  $\mathrm{Eu}^{3+}$  in BAM, a reduction effect of Eu<sup>3+</sup> to Eu<sup>2+</sup> is observed in C@BAM-700 °C with remained 1-2 carbon layers, contributing to its superior PL performance. Present research on the evolution of carbon layer-Eu valenceluminescent properties triggers a potential strategy to improve the performance of other carbon coated phosphors.

#### Acknowledgments

This research was supported by the National Natural Science Foundation of China (Grant No. 51302029 and 51402040) and the Fundamental Research Funds for the Central Universities (Grant No. ZYGX2015J110). Especially, the authors thank Yi-Fei Wang for providing the XANES result of BaMgAl $_{10}$ O $_{17}$ : Eu $^2$ + at room temperature, performed in the National Synchrotron Radiation Laboratory of China, and thank Shanghai Synchrotron Radiation Facility for providing the XANES measurements of the other samples.

#### Appendix A. Supporting information

Supplementary data associated with this article can be found in the online version at http://dx.doi.org/10.1016/j.ceramint.2018.02.080.

#### References

[1] S. Zhang, T. Kono, A. Ito, T. Yasaka, H. Uchiike, Degradation mechanisms of the blue-emitting phosphor BaMgAl<sub>10</sub>O<sub>17</sub>: Eu<sup>2+</sup> under baking and VUV-irradiating

- treatments, J. Lumin. 106 (2004) 39-46.
- [2] B. Moine, G. Bizarri, Why the quest of new rare earth doped phosphors deserves to go on, Opt. Mater. 28 (2006) 58–63.
- [3] T. Justel, J.C. Krupa, D.U. Wiechert, VUV spectroscopy of luminescent materials for plasma display panels and Xe discharge lamps, J. Lumin. 93 (2001) 179–189.
- plasma display panels and Xe discharge lamps, J. Lumin. 93 (2001) 179–189. [4] G. Bizarri, B. Moine, On BaMgAl<sub>10</sub>O<sub>17</sub>: Eu<sup>2+</sup> phosphor degradation mechanism: thermal treatment effects, J. Lumin. 113 (2005) 199–213.
- [5] Y.F. Wang, X. Xu, L.J. Yin, L.Y. Hao, High thermal stability and photoluminescence of Si-N-codoped BaMgAl<sub>10</sub>O<sub>17</sub>: Eu<sup>2+</sup> phosphors, J. Am. Ceram. Soc. 93 (2010) 1534–1536.
- [6] K.B. Kim, K.W. Koo, T.Y. Cho, H.G. Chun, Effect of heat treatment on photoluminescence behavior of BaMgAl<sub>10</sub>O<sub>17</sub>: Eu<sup>2+</sup> phosphors, Mater. Chem. Phys. 80 (2003) 682–689.
- [7] B. Howe, A.L. Diaz, Characterization of host-lattice emission and energy transfer in  ${\rm BaMgAl_{10}O_{17}}$ :  ${\rm Eu^{2}}^+$ , J. Lumin. 109 (2004) 51–59.
- [8] C.W. Yeh, W.T. Chen, R.S. Liu, S.F. Hu, H.S. Sheu, J.M. Chen, H.T. Hintzen, Origin of thermal degradation of Sr<sub>2-x</sub>Si<sub>5</sub>N<sub>8</sub>: Eu<sub>x</sub> phosphors in air for light-emitting diodes, J. Am. Chem. Soc. 134 (2012) 14108–14117.
- [9] C.Y. Wang, R.J. Xie, F. Li, X. Xu, Thermal degradation of the green-emitting SrSi<sub>2</sub>O<sub>2</sub>N<sub>2</sub>: Eu<sup>2+</sup> phosphor for solid state lighting, J. Mater. Chem. C 2 (2014) 2735–2742.
- [10] Y.-F. Wang, Y.-F. Wang, J.-K. Gao, M.-H. Lee, W. He, X. Xu, L.-Y. Hao, J.-H. Chen, First-principles study on enhanced optical stability of BaMgAl<sub>10</sub>O<sub>17</sub>: Eu<sup>2+</sup> phosphor by SiN doping, Chin. J. Chem. Phys. 25 (2012) 398–402.
- [11] B. Liu, Y. Wang, J. Zhou, F. Zhang, Z. Wang, The reduction of Eu<sup>3+</sup> to Eu<sup>2+</sup> in BaMgAl<sub>10</sub>O<sub>17</sub>: Eu and the photoluminescence properties of BaMgAl<sub>10</sub>O<sub>17</sub>: Eu<sup>2+</sup> phosphor, J. Appl. Phys. 106 (2009) 053102.
- [12] B. Liu, Y. Wang, F. Zhang, Y. Wen, Q. Dong, Z. Wang, Thermal stability and photoluminescence of S-doped BaMgAl<sub>10</sub>O<sub>17</sub>: Eu<sup>2+</sup> phosphors for plasma display panels, Opt. Lett. 35 (2010) 3072–3074.
- [13] C. Liang, C. Zhang, Y. Dong, T. Cao, J. Jiang, J. He, Improving thermal stability of BaMgAl<sub>10</sub>O<sub>17</sub>: Eu phosphor, J. Rare Earth 24 (2006) 153–156.
- [14] K.Y. Jung, D.Y. Lee, Y.C. Kang, Improved thermal resistance of spherical BaMgAl<sub>10</sub>O<sub>17</sub>: Eu blue phosphor prepared by spray pyrolysis, J. Lumin. 115 (2005) 91–96.
- [15] S. Ekambaram, K.C. Patil, Synthesis and properties of Eu<sup>2+</sup> activated blue phosphors, J. Alloy. Compd. 248 (1997) 7–12.
- [16] Z. Chen, Y.W. Yan, J.-M. Liu, Y. Yin, H. Wen, G. Liao, C. Wu, J. Zao, D. Liu, H. Tian, C. Zhang, S. Li, Microstructure and luminescence of surface-coated nano-BaMgAl<sub>10</sub>O<sub>17</sub>: Eu<sup>2+</sup> blue phosphor, J. Alloy. Compd. 478 (2009) 679–683.
  [17] H. Zhu, H. Yang, W. Fu, P. Zhu, M. Li, Y. Li, Y. Sui, S. Liu, G. Zou, The improvement
- [17] H. Zhu, H. Yang, W. Fu, P. Zhu, M. Li, Y. Li, Y. Sui, S. Liu, G. Zou, The improvement of thermal stability of BaMgAl<sub>10</sub>O<sub>17</sub>: Eu<sup>2+</sup> coated with MgO, Mater. Lett. 62 (2008) 784–786
- [18] X.M. Teng, W. Zhuang, X. Huang, X. Cui, S. Zhang, Luminescent properties of BaMgAl<sub>10</sub>O<sub>17</sub>: Eu<sup>2+</sup> phosphors coated with Y<sub>2</sub>SiO<sub>5</sub>, J. Rare Earth 24 (2006) 143–145.
- [19] F. Li, Y. Yang, Y. Song, W. Wang, W. Yang, B. Yang, Photoluminescence spectroscopic study of BaMgAl<sub>10</sub>O<sub>17</sub>: Eu phosphor coated with CaF<sub>2</sub> via a sol-gel process, J. Spectrosc. (2013), http://dx.doi.org/10.1155/2013/312519.
- [20] R.R. Nair, P. Blake, A.N. Grigorenko, K.S. Novoselov, T.J. Booth, T. Stauber, N.M.R. Peres, A.K. Geim, Fine structure constant defines visual transparency of graphene, Science 320 (2008) (1308-1308).
- [21] K.S. Kim, Y. Zhao, H. Jang, S.Y. Lee, J.M. Kim, K.S. Kim, J.-H. Ahn, P. Kim, J.-Y. Choi, B.H. Hong, Large-scale pattern growth of graphene films for stretchable transparent electrodes, Nature 457 (2009) 706–710.
- [22] L.-J. Yin, J. Dong, Y. Wang, B. Zhang, Z.-Y. Zhou, X. Jian, M. Wu, X. Xu, J.R. Ommen, T. Hubertus Hintzen, Enhanced optical performance of BaMgAl<sub>10</sub>O<sub>17</sub>: Eu<sup>2+</sup> phosphor by a novel method of carbon coating, J. Phys. Chem. C 120 (2016) 2355–2361.
- [23] T. Ishigaki, H. Mizushina, K. Uematsu, N. Matsushit, M. Yoshimura, K. Toda, M. Sato, Microwave synthesis technique for long phosphorescence phosphor SrAl<sub>2</sub>O<sub>4</sub>: Eu<sup>2+</sup>, Dy<sup>3+</sup> using carbon reduction, Mater. Sci. Eng. B-Adv. 173 (2010) 109–112.
- [24] C. Zhang, T. Uchikoshi, R.-J. Xie, L. Liu, Y. Cho, Y. Sakka, N. Hirosaki, T. Sekiguchi, Reduced thermal degradation of the red-emitting  $\rm Sr_2Si_5N_8$ :  $\rm Eu^{2+}$  phosphor via thermal treatment in nitrogen, J. Mater. Chem. C 3 (2015) 7642–7651.